

# Path Integral Monte Carlo on a Sphere

Riccardo Fantoni\*

*Università di Trieste, Dipartimento di Fisica, strada Costiera 11, 34151 Grignano (Trieste), Italy*

(Dated: March 4, 2026)

We solve numerically exactly a simple toy model to quantum general relativity or more properly to path integral on a curved space. we consider the thermal equilibrium of a quantum many body problem on the sphere, the surface of constant positive curvature. We use path integral Monte Carlo to measure the kinetic energy, the internal energy and the static structure of a bosons, fermions and anyons fluid at low temperatures on the sphere. For bosons we also measure the superfluid fraction and confirm its universal jump at the superfluid transition, as predicted by Nelson and Kosterlitz. For fermions and anyons it is necessary to use the restricted path integral recipe in order to overcome the sign problem. Even if this recipe is exact for the non interacting fluid it resorts to just an approximation for an interacting system. And we make the example of the electron gas at low temperature. Snapshots of the many body path configuration during the evolution of the computer experiment show that the “speed” of the single particle path near the poles slows down as a consequence of the “hairy ball theorem” of Poincaré.

Keywords: Path Integral; Monte Carlo; Sphere; Quantum Fluid; Bosons; Fermions; Anyons; Thermodynamics; Structure; Superfluidity; Sign Problem

## CONTENTS

I. Introduction	2
II. Many body path integral on a Riemannian manifold	2
III. The sphere	5
IV. Non interacting bodies	6
A. Distinguishable bodies	7
B. Identical bodies	7
Bosons	8
Fermions	9
Anyons	10
V. Electron gas	12
VI. Conclusions	12
A. The transition displacement move	13
B. The transition bridge move	14
C. Braids sampling	14
Author declarations	15
Conflicts of interest	15
Data availability	15
Funding	15
References	15

---

\* [riccardo.fantoni@scuola.istruzione.it](mailto:riccardo.fantoni@scuola.istruzione.it)

## I. INTRODUCTION

One of the greatest challenges of today physics is the problem of putting together the quantum theory with the general relativity theory, or from the mathematical side we are looking forward to a bridge between the functional integral underlying a Hilbert space and the Riemannian manifold underlying differential geometry or more generally differential topology. We are still at the beginning of this ambitious project and from this point of view any simple, yet well defined, physical model at the interception of these two theories is certainly valuable, especially so if the model can be solved exactly from a mathematical point of view [1, 2].

Guided by this motivation some years ago we studied the statistical physics problem of an electron gas at finite non zero temperature on the surface of a sphere [3, 4], the surface of constant positive curvature and probably the simplest of all Riemannian manifolds. Similar studies on the Haldane sphere had already been tried but at zero temperature [5–7]. And at high temperature, at a special value of the Coulomb coupling constant, in the non quantum regime on several different (curved) surfaces: the plane [8–11], the cylinder [12, 13], the sphere [14–17], the pseudosphere [18–20], and the Flamm paraboloid [21, 22].

Here we want to examine carefully the case of a many body system on a sphere at finite non zero low temperature, in its quantum regime.

The bodies that form the statistical physics model can be described either as distinguishable or as identical. In their description as identical bodies we can further distinguish between whether they obey to Bose-Einstein statistics or if they obey to Fermi-Dirac statistics according to their wave function transformation property under their permutation. If additionally they are described as identical and impenetrable bodies they will obey to anyonic statistics according to their wave function imaginary time braiding evolution. The braid group was introduced in 1925 by Emil Artin [23]. Their thermal equilibrium properties at low temperature will be captured by a path integral description of their density matrix. All these descriptions bring to different statistical physics and thermodynamic properties when the many body system is in its low temperature quantum regime, and they merge at high temperature [24].

On the other side already the simple sphere has some quite delicate features as for example the *hairy ball theorem*, according to which her Euler class is the obstruction to her tangent plane having always a non vanishing *fiber*, or hair, for any *section*<sup>1</sup>. The theorem was first proven by Henri Poincaré for the sphere in 1885 [25], and extended to higher even dimensions in 1912 by Luitzen Egbertus Jan Brouwer [26]. The theorem has been expressed colloquially as “you can’t comb a hairy ball flat without creating a cowlick”. If  $f$  is a continuous function that assigns a vector in the three dimensional space to every point  $\mathbf{r}$  on a sphere such that  $f(\mathbf{r})$  is always tangent to the sphere at  $\mathbf{r}$ , then there is at least one pole, a point where the field vanishes, i.e. an  $\mathbf{r}$  such that  $f(\mathbf{r}) = 0$ . Every zero of a vector field has a (non-zero) *index*<sup>2</sup>, and it can be shown that the sum of all of the indexes at all of the zeros must be two, because the Euler characteristic of the sphere is two. Therefore, there must be at least one zero. This is a consequence of the *Poincaré-Hopf theorem*. The theorem was proven for two dimensions by Henri Poincaré and later generalized to higher dimensions by Heinz Hopf [27]. In particular we expect that even a single free particle in thermal equilibrium at low temperature on the sphere have a path which will be subject to some peculiar topological features [28].

The question of the influence on the statistical physics properties of a quantum many body fluid of the curvature of the supporting Riemannian surface is not straightforward. In fact already for a single free particle the phase space dynamics on a sphere is generally not ergodic since her trajectories, the geodesics, may be confined to invariant tori, but the picture dramatically changes on a pseudosphere, as was proven by Emil Artin in 1924 [29], where geodesics diverge [19]. This makes the quantum version of this system a paradigmatic model of quantum chaos.

We then here plan to study this preliminary simple toy model of a quantum many body fluid on a sphere, which nonetheless does not allow for an analytic exact solution, with the instrument of Path Integral Monte Carlo (PIMC) [30] which is able to extract exact numerical properties of the statistical physics model. It certainly is gratifying to know that at least this simple toy model of statistical general relativity [31–33] can be solved exactly even if only numerically.

## II. MANY BODY PATH INTEGRAL ON A RIEMANNIAN MANIFOLD

Throughout the whole paper we will denote with a bold face letter a point on the  $d$  dimensional Riemannian manifold  $\mathcal{M}$ . Greek indexes run over the  $d$  space dimensions. Roman indexes are used either for a particle label and

<sup>1</sup> In topology, a cross *section* of a *fiber* (tangent) *bundle* space,  $B \times F$ , in this case the sphere, is a graph over the *base space*  $B$ , in this case the tangent vectors. A tangent vector to any point of the sphere is a section of the tangent bundle of the sphere.

<sup>2</sup> The index of a bilinear function/al is the dimension of the space on which it is negative definite. In the context of vector fields on a Riemannian manifold the index is equal to +1 around a source or a sink, and more generally equal to  $(-1)^k$  around a saddle that has  $k$  contracting dimensions and  $n - k$  expanding dimensions.

for an imaginary timeslice label in the path integral discretization. We use Einstein summation convention of tacitly assuming a sum over repeated greek indexes.

A many body system is composed of  $N$  *distinguishable* particles of mass  $m$  and spin  $s$  with positions in  $R = (\mathbf{r}_1, \mathbf{r}_2, \dots, \mathbf{r}_N) = (\{\mathbf{r}_i\})$  where each position vector  $\mathbf{r}_i = (r_i^1, r_i^2, \dots, r_i^d) = (\{r_i^\alpha\})$  in  $d$  dimensions. On a Riemannian manifold  $\mathcal{M}$  of dimension  $d$  and metric tensor  $g_{\alpha\beta}(\mathbf{r})$ , the geodesic distance between two infinitesimally close points  $R$  and  $R'$  is  $d\tilde{s}^2(R, R') = \sum_{i=1}^N ds^2(\mathbf{r}_i, \mathbf{r}'_i)$  where  $ds^2(\mathbf{r}, \mathbf{r}') = g_{\alpha\beta}(\mathbf{r})(\mathbf{r} - \mathbf{r}')^\alpha(\mathbf{r} - \mathbf{r}')^\beta$ . Moreover,

$$\tilde{g}_{\mu\nu}(R) = g_{\alpha_1\beta_1}(\mathbf{r}_1) \otimes \dots \otimes g_{\alpha_N\beta_N}(\mathbf{r}_N), \quad (2.1)$$

$$\tilde{g}(R) = \prod_{i=1}^N \det \|g_{\alpha_i\beta_i}(\mathbf{r}_i)\|, \quad (2.2)$$

where  $\|\tilde{g}_{\mu\nu}\|$  is a matrix made of  $N$  diagonal blocks  $\|g_{\alpha_i\beta_i}\|$  with  $i = 1, 2, \dots, N$ . The Laplace-Beltrami operator on the manifold of dimension  $dN$  is

$$\Delta_R = \tilde{g}^{-1/2} \nabla_\mu (\tilde{g}^{1/2} \tilde{g}^{\mu\nu} \nabla_\nu), \quad (2.3)$$

where  $\nabla = \nabla_R$ ,  $\tilde{g}^{\gamma\nu}$  is the inverse of  $\tilde{g}_{\gamma\nu}$ , i.e.  $\tilde{g}_{\mu\gamma} \tilde{g}^{\gamma\nu} = \delta_\mu^\nu$  the Kronecker delta, and a sum over repeated indexes is tacitly assumed.

We will first assume *free*, non interacting bodies, with an Hamiltonian  $\mathcal{H}$  that reduces to the one of the free gas in flat space. For the sake of simplicity <sup>3</sup> we will choose

$$\mathcal{H} = -\lambda \Delta_R, \quad (2.4)$$

with  $\lambda = \hbar^2/2m$ .

For *interacting* bodies we will then have more generally

$$\mathcal{H} = -\lambda \Delta_R + V(R), \quad (2.5)$$

where  $V$  is the potential energy of the system, that we here assume only a function of the particles positions and bounded from below.

The density matrix  $\rho$  of the system obeys Bloch equation

$$\frac{\partial \rho(t)}{\partial t} = -\mathcal{H} \rho(t), \quad (2.6)$$

$$\rho(0) = \mathbb{1}, \quad (2.7)$$

where  $t$  is the imaginary time with the dimensions of an energy and  $\mathbb{1}$  the identity matrix. The position representation of the density matrix is then obtained from  $\rho(R, R'; t) = \langle R | \rho(t) | R' \rangle$  with  $\langle R | R' \rangle = \delta(R - R') / \sqrt{\tilde{g}(R)}$  where  $\delta$  is a  $dN$  dimensional Dirac delta function. In the small imaginary time  $\tau$  limit the position representation of the density matrix is

$$\rho(R, R'; \tau) \propto \tilde{g}(R)^{-1/4} \sqrt{\mathcal{D}(R, R'; \tau)} \tilde{g}(R')^{-1/4} e^{\lambda \tau \mathcal{R}(R)/6} e^{-\mathcal{S}(R, R'; \tau)}, \quad (2.8)$$

where  $\mathcal{R}$  is the scalar curvature of the manifold <sup>4</sup>,  $\mathcal{S}$  the action, and  $\mathcal{D}$  the van Vleck's determinant [35, 36]

$$\mathcal{D}_{\mu\nu} = -\nabla_\mu \nabla'_\nu \mathcal{S}(R, R'; \tau), \quad (2.9)$$

$$\det \|\mathcal{D}_{\mu\nu}\| = \mathcal{D}(R, R'; \tau), \quad (2.10)$$

where  $\nabla = \nabla_R$  and  $\nabla' = \nabla_{R'}$ . This determinant is the Jacobian of the transformation from the initial conditions given by fixing the pair of momentum and coordinate to the boundary conditions given by specifying the pair of initial and final coordinates needed in the path integral formulation. For the density matrix (2.8) the volume element for integration is  $\sqrt{\tilde{g}(R)} dR$ . The two factors  $\tilde{g}^{-1/4}$  are needed in order to have for the density matrix a bidensity for which the boundary condition to Bloch equation is simply a Dirac delta function  $\rho(R, R'; 0) = \delta(R - R')$ . The square root of the van Vleck determinant factor takes into account the density of paths among the minimum extremal region for the action (see Chapter 12 of Ref. [36]).

<sup>3</sup> This is a delicate point and should be studied more carefully [1]. Especially for what concerns ordering ambiguities. We here appeal to simplicity.

<sup>4</sup> The factor depending on the curvature of the manifold is due to Bryce DeWitt [34]. For a space of constant curvature there is clearly no effect, as the term due to the curvature just leads to a constant multiplicative factor that has no influence on the measure of the various observables.

For the *action*  $\mathcal{S}$ , the *kinetic-action*  $\mathcal{K}$ , and the *inter-action*  $\mathcal{U}$  we have <sup>5</sup>

$$\mathcal{S}(R, R'; \tau) = \mathcal{K}(R, R'; \tau) + \mathcal{U}(R, R'; \tau), \quad (2.11)$$

$$\mathcal{K}(R, R'; \tau) = \frac{dN}{2} \ln(4\pi\lambda\tau) + \frac{d\tilde{s}^2(R, R')}{4\lambda\tau}. \quad (2.12)$$

In particular the kinetic-action is responsible for a diffusion of the random walk with a single particle variance on the  $\alpha, \beta$  components equal to  $\sigma_{\alpha\beta}^2(\mathbf{r}) = 2\lambda\tau/g_{\alpha\beta}(\mathbf{r})$ . The inter-action is defined as  $\mathcal{U} = \mathcal{S} - \mathcal{K}$  and for potential energies bounded from below one can resort to Trotter formula [37] to reach the *primitive approximation* <sup>6</sup>

$$\mathcal{U}(R, R'; \tau) = \tau[V(R) + V(R')]/2. \quad (2.13)$$

For non interacting bodies  $\mathcal{U} = 0$ . Note that, even to lowest order in  $R - R'$  <sup>7</sup>, the path integral in the curved manifold for the non interacting system will not coincide with the one in flat space since it is not possible with a change of coordinates to simply remove the metric factor from both  $d\tilde{s}^2$  and the volume element of integration, if not only locally. In fact this would require a *non coordinate basis* [38].

Given then an observable  $\mathcal{O}$  we can determine its thermal average at an absolute temperature  $T$  from

$$\langle \mathcal{O} \rangle = g_s \text{tr}\{\rho(\beta)\mathcal{O}\}/Z_N, \quad (2.14)$$

$$Z_N = g_s \text{tr}\{\rho(\beta)\}, \quad (2.15)$$

where  $\beta = 1/k_B T$  with  $k_B$  Boltzmann constant,  $\text{tr}\{\dots\}$  is the trace over the spatial variables,  $Z_N$  the canonical partition function,  $g_s = 2s + 1$  is the spin degeneracy, and we assumed the Hamiltonian independent from spin. *Spinless* bodies have  $g_s = 1$ . Actually the spin-statistics theorem of quantum field theory, dictates that in spatial dimension bigger than two, particles with integer spin are bosons (obeying Bose-Einstein statistics, symmetric wavefunctions), while half-integer spin particles are fermions (obeying Fermi-Dirac statistics, antisymmetric wavefunctions). In dimension two anyonic statistics are also possible.

The position representation of the density matrix at an imaginary time  $t = \beta$  is obtained through a path integral

$$\rho(R, R'; \beta) = \langle R|\rho(\beta)|R' \rangle = \int \prod_{k=0}^{M-1} [\rho(R_k, R_{k+1}; \tau) dR_k] \delta(R_0 - R) \delta(R_M - R') dR_M, \quad (2.16)$$

where we have discretized the imaginary time  $\beta$  into  $M$  *timeslices* with a small *timestep*  $\tau = \beta/M$ , a *bead*  $R_k = (\{\mathbf{r}_{i,k}\}) = (\{r_{i,k}^\alpha\})$  at each timeslice  $k = 1, 2, \dots, M$ . We will also call *link* a pair of contiguous beads. Note that in order to measure an observable through Eq. (2.14) it is necessary to consider closed paths such that  $R(t + \beta) = R(t)$ , or rings on the manifold  $\mathcal{M}$ .

For *identical* bodies if they satisfy to the Bose-Einstein statistics one needs to symmetrize the distinguishable density matrix, if they satisfy to the Fermi-Dirac statistics one needs to antisymmetrize it [39]. In these cases we can then write <sup>8</sup>

$$\rho_{\pm}(R, R'; \beta) = \frac{1}{N!} \sum_{\mathcal{P}} \text{sgn}(\mathcal{P}) \rho(\mathcal{P}R, R'; \beta), \quad (2.17)$$

$$\text{sgn}(\mathcal{P}) = (\pm 1)^{\sum_{\nu=1}^N (\nu-1)C_{\nu}}, \quad (2.18)$$

where  $\mathcal{P}$  is any permutation of the  $N$  particles such that  $\mathcal{P}R = (\mathbf{r}_{\mathcal{P}1}, \mathbf{r}_{\mathcal{P}2}, \dots, \mathbf{r}_{\mathcal{P}N})$ , with sign  $\text{sgn}(\mathcal{P})$ . Any permutations can be broken into cycles  $\mathcal{P} = \{C_{\nu}\}$  where  $C_{\nu}$  is the number of cycles of length  $\nu$  in  $\mathcal{P}$ . In the sum over the permutation one should use a +1 for the symmetrization necessary for bosons and -1 for the antisymmetrization necessary for fermions, in  $\text{sgn}(\mathcal{P})$ . An even (odd) permutation has  $\text{sgn}(\mathcal{P}) = +1(-1)$  and an even (odd) number of exchanges of a pair of particles.

On a surface,  $d = 2$ , for *impenetrable* identical bodies, one can also have anyonic statistics [40]. In this case it is necessary to consider, more generally,

$$\rho_{\nu}(R, R'; \beta) = \sum_{\alpha \in B_N} \text{Re}[\chi(\alpha)] \rho_{\alpha}(R, R'; \beta), \quad (2.19)$$

$$\chi(\{\text{paths } R(t) \text{ with } n \text{ braids among the pairs of single particle paths } \mathbf{r}(t)\}) = e^{-i\nu n\pi}, \quad (2.20)$$

<sup>5</sup> The expression for  $\mathcal{K}$  is the one of Eq. (24.16) of Ref. [36] to lowest order in  $R - R'$ .

<sup>6</sup> See Ref. [30] for a numerical analysis of the accuracy of this approximation and for possible its refinements.

<sup>7</sup> For next orders corrections see for example Ref. [28].

<sup>8</sup> One can symmetrize or antisymmetrize respect to the first, the second or both the arguments of the distinguishable density matrix. We here choose the first case.

where  $B_N$  is the infinite braid group which admits an infinite number of unitary one dimensional representations  $\chi$  parametrized by an arbitrary number  $\nu$  which determines the statistics and  $\rho_\alpha$  is the distinguishable density matrix obtained from paths of kind  $\alpha$  only. Clearly for  $\nu = 0$  (modulo 2) we recover the Bose-Einstein statistics and for  $\nu = 1$  (modulo 2) the Fermi-Dirac statistics. So we will be interested in values of  $0 < \nu < 1$ .

The braid group is the fundamental group of the quotient space  $(S^{2N} - \Delta)/S_N$  where  $S^2$  is the (two) sphere,  $\Delta = \{R \mid \mathbf{r}_i = \mathbf{r}_j \text{ for some } i \neq j\}$ , and  $S_N$  is the group of permutation of  $N$  bodies. We then see how paths  $R(t)$  with different numbers of crossings between single particle paths  $\mathbf{r}(t)$  belong to different homotopy classes and one cannot be deformed continuously into the other. Therefore in order to take care of the density matrix of identical impenetrable bodies it is necessary to sum over all the topologically disjoint homotopy classes as is done in Eq. (2.19). If  $\nu$  is rational, i.e. for *fractional statistics* the phase factor will be periodic and for irrational  $\nu$  not.

### III. THE SPHERE

A sphere of radius  $a$  is the surface,  $d = 2$ <sup>9</sup>, with metric  $ds^2 = g_{\alpha\beta} dr^\alpha dr^\beta = a^2(d\theta^2 + \cos^2\theta d\varphi^2)$ ,<sup>10</sup> of constant positive scalar curvature  $2/a^2$  so that  $\mathcal{R} = 2N/a^2$ . The polar angle  $r^1 = \theta \in ] - \pi/2, \pi/2]$  and the azimuthal angle  $r^2 = \varphi \in ] - \pi, \pi]$  are the contravariant coordinates of the position vector  $\mathbf{r} \in \mathcal{C}$  with  $\mathcal{C} = ] - \pi/2, \pi/2] \times ] - \pi, \pi]$  the single particle positions space. On the sphere  $\sqrt{g(\mathbf{r})} = a^2 |\cos\theta|$  and in the small  $\tau \rightarrow 0$  limit<sup>11</sup>  $\tilde{g}(R)^{-1/4} \sqrt{D(R, R'; \tau)} \tilde{g}(R')^{-1/4} \rightarrow (1/2\lambda\tau)^N$ . So we see how both the curvature term and the van Vleck factor, being constant, simply drop off from the measure of the various observables of Eq. (2.14).

The position of a particle on the sphere in the three dimensional Euclidean space embedding the sphere is

$$\begin{cases} x = a \cos \theta \cos \varphi \\ y = a \cos \theta \sin \varphi \\ z = a \sin \theta \end{cases} \quad (3.1)$$

and the particle path in it is  $\mathbf{q}(t) = (x(t), y(t), z(t))$ .

The geodesic distance between particles  $\mathbf{r}_i$  and  $\mathbf{r}_j$  is

$$s_{ij} = s(\mathbf{r}_i, \mathbf{r}_j) = a \arccos [\sin(r_i^1) \sin(r_j^1) + \cos(r_i^1) \cos(r_j^1) \cos(r_i^2 - r_j^2)], \quad (3.2)$$

whereas the Euclidean distance is

$$d_{ij} = d(\mathbf{r}_i, \mathbf{r}_j) = a \sqrt{2(1 - \hat{\mathbf{q}}_i \cdot \hat{\mathbf{q}}_j)} = 2a \sin[\arccos(\hat{\mathbf{q}}_i \cdot \hat{\mathbf{q}}_j)/2], \quad (3.3)$$

where  $\hat{\mathbf{q}}_i = \mathbf{q}_i/a$  is the versor that from the center of the sphere points towards the center of the  $i$ th particle.

We use the Metropolis algorithm [41, 42] to evaluate the average of Eq. (2.14).

In order to explore ergodically the positions space  $\mathbf{r} = (\theta, \varphi) \in \mathcal{R}$  to sample the distinguishable density matrix we use the transition *displacement* move described in Appendix A.

In order to sample the permutation sum of Eq. (2.17) needed for identical bodies we use a transition move combination of 2 Brownian *bridges* between unlike bodies as described in Appendix B. To construct a single Brownian bridge it is essential to map, project, the sphere on a flat coordinate system. Our choice is presented in Appendix B. Perform the Gaussian bridge move in the projection flat space and then map it back to the sphere. The Metropolis algorithm will then allow to sample the high temperature density matrix whose kinetic action is not purely Gaussian on the sphere, due to the metric tensor appearing in  $d\tilde{s}^2$ <sup>12</sup>.

In order to sample the sum over the homotopy classes of Eq. (2.19) needed for identical (impenetrable) bodies we use a combination of bridge and displacement transition moves as described in Appendix C. Note that the displacement moves can be freely substituted by moves of bridges connecting only like bodies. But we found it convenient to use both moves for three reasons: (i) a Monte Carlo method usually becomes more efficient if implemented through a rich menu of different moves; (ii) from a purely formal point of view where one starts from simple single bead moves and only later builds more complex many beads moves; (iii) since the single bead displacement move is simple to construct it can serve as a test for more elaborated many beads moves.

We will work in the canonical ensemble with fixed number of particles  $N$ , surface area  $A = 4\pi a^2$ , surface density  $\sigma = N/4\pi a^2$ , and absolute temperature  $T = 1/k_B\beta$ . In our simulations we will only consider the  $m = 1$  case. The

<sup>9</sup> So it is conformally flat as any Riemannian manifold of dimension  $d \leq 3$ .

<sup>10</sup> Note that in the kinetic action of the path integral Monte Carlo calculation it is crucial to use consistently either  $ds^2(\mathbf{r}, \mathbf{r}') = g_{\alpha\beta}(\mathbf{r})(\mathbf{r} - \mathbf{r}')^\alpha (\mathbf{r} - \mathbf{r}')^\beta$  or  $ds^2(\mathbf{r}, \mathbf{r}') = g_{\alpha\beta}(\mathbf{r}')(\mathbf{r} - \mathbf{r}')^\alpha (\mathbf{r} - \mathbf{r}')^\beta$ .

<sup>11</sup> Remember that the metric tensor is covariantly constant.

<sup>12</sup> We tried to avoid passing back and forth through the projection mapping but with no results. In fact in order to be able to construct a Brownian bridge it is necessary to connect particles several timeslices apart. And their geodesic distance  $s_{ij}$  does not reduce to a simple quadratic form.

many body system *degeneracy parameter* is  $\Theta = T/T_D$  where the degeneracy temperature  $T_D = \sigma \hbar^2/mk_B$ . For temperatures higher than  $T_D$ ,  $\Theta \gg 1$ , quantum effects are less relevant. We will treat both the non interacting fluid  $V = 0$  and the Coulomb fluid

$$V(R) = \sum_{i < j} \frac{e^2}{d_{ij}}, \quad (3.4)$$

where  $e$  is the unit of charge and we are assuming that the particles, moving on the sphere, interact with the three dimensional pair Coulomb potential in terms of the Euclidean distance (3.3)<sup>13</sup>. The *Coulomb coupling constant* is  $\Gamma = \beta e^2/a_0 r_s$  with  $a_0 = \hbar^2/me^2$  the Bohr radius and the Wigner-Seitz radius  $r_s = (4\pi\sigma)^{-1/2}/a_0$ . At weak coupling,  $\Gamma \ll 1$ , the plasma becomes weakly correlated and approach the ideal gas limit. This will occur at high temperature and/or low density.

Choosing length in units of Wigner-Seitz radius,  $a_0 r_s = a/\sqrt{N}$ , and energy in units of Rydberg,  $\text{Ry} = \hbar^2/2ma_0^2$ , we have  $\lambda = \text{Ry}/r_s^2$ ,  $\Gamma = \beta(2/r_s)$ , and  $\Theta = (2\pi r_s^2)/\beta$ . In this work we will choose units so that  $\hbar = k_B = 1$ .

Apart from the *kinetic energy* per particle  $e_K$  and the *potential energy* per particle  $e_V$ <sup>14</sup> we will also measure the *radial distribution function*,  $g(r) = \langle \mathcal{O} \rangle$  for which we may use the following histogram estimator,

$$O(R; r) = \sum_{i \neq j} \frac{1_{]r-\Delta/2, r+\Delta/2]}(d_{ij})}{N n_{id}(r)}, \quad (3.5)$$

where  $\Delta$  is the histogram bin,  $1_{]a,b]}(x) = 1$  if  $x \in ]a, b]$  and 0 otherwise, and

$$n_{id}(r) = N \left[ \left( \frac{r + \Delta/2}{2a} \right)^2 - \left( \frac{r - \Delta/2}{2a} \right)^2 \right], \quad (3.6)$$

is the average number of particles on the spherical crown  $]r - \Delta/2, r + \Delta/2]$  for the ideal gas of density  $\sigma$ . We have that  $\sigma^2 g(r)$  gives the probability, that sitting on a particle at  $\mathbf{r}$ , one finds another particle at  $\mathbf{r}'$  with  $r = d(\mathbf{r}, \mathbf{r}') \in [0, 2a]$ . Note that  $\sqrt{2a^2}$  is the Euclidean distance between a pole and a point on the equator. Alternatively one could consider a radial distribution function defined through the geodesic distance  $r = s(\mathbf{r}, \mathbf{r}') \in [0, \pi a]$  where one chooses  $1_{]r-\Delta/2, r+\Delta/2]}(s_{ij})$  in Eq. (3.5) with an appropriate normalization<sup>15</sup>.

For  $e_K$  and  $e_V$  we will use the *direct* estimator described in Ref. [30] applied to our action of Eq. (2.11).

In Table I we list some case studies treated by our computer experiments.

TABLE I. Cases treated in our simulations:  $a$  the sphere radius,  $N$  the number of particles,  $\beta$  the inverse temperature,  $e_K = \langle \mathcal{K} \rangle$  the kinetic energy per particle from the thermodynamic estimator as explained in Ref. [30], and  $e_V = \langle \mathcal{V} \rangle$  the potential energy per particle. The other quantities were introduced in the main text. In the statistics column ‘‘D’’ stands for distinguishable, ‘‘B’’ for bosons, ‘‘F’’ for fermions, and a nombre  $\nu \in ]0, 1[$  for anyons. We chose units with  $\hbar = k_B = 1$ .

case	statistics	$M$	$N$	$a$	$a/\sqrt{N}$	$\beta$	$\Gamma$	$\Theta$	$e_K$	$e_V$
A	D	50	10	5	1.581	10	0	$\pi$	1.094(3)	0
B	B $\nu = 0$	50	10	5	1.581	100/3	0	$3\pi/10$	0.222(2)	0
C	F $\nu = 1$	50	10	5	1.581	100/3	0	$3\pi/10$	0.919(8)	0
D	$\nu = 1/2$	50	10	5	1.581	100/3	0	$3\pi/10$	0.910(9)	0
E	F $\nu = 1$	50	10	5	1.581	100/3	$6.324 \times e^2$	$3\pi/10$	1.154(8)	7.066(2)
...										

#### IV. NON INTERACTING BODIES

Here we will study non interacting spinless,  $s = 0$ , bodies with  $\Gamma = 0$  or more generally  $V = 0$ .

<sup>13</sup> Note that this is not the only possible choice since we could as well choose particles ‘‘living in’’ [43] the surface of the sphere as done for example in Ref. [19, 21, 22] (for other surfaces) or particle ‘‘moving on’’ the sphere but interacting with the two dimensional logarithmic Coulomb potential with the Euclidean distance as done for example in Ref. [14, 44].

<sup>14</sup> The estimators for these observables are carefully described in Ref. [30].

<sup>15</sup> In Ref. [3] we used the Euclidean distance.

### A. Distinguishable bodies

Here we use the Metropolis algorithm with the transition displacement moves of Eqs. (A1) and (A2) or equivalently bridge moves of Eqs. (B1) and (B2) but between like particles.

In Fig. 1 we show a snapshot during the simulation for distinguishable non interacting particles with  $M = 50, N = 10, a = 5, \beta = 10$ .

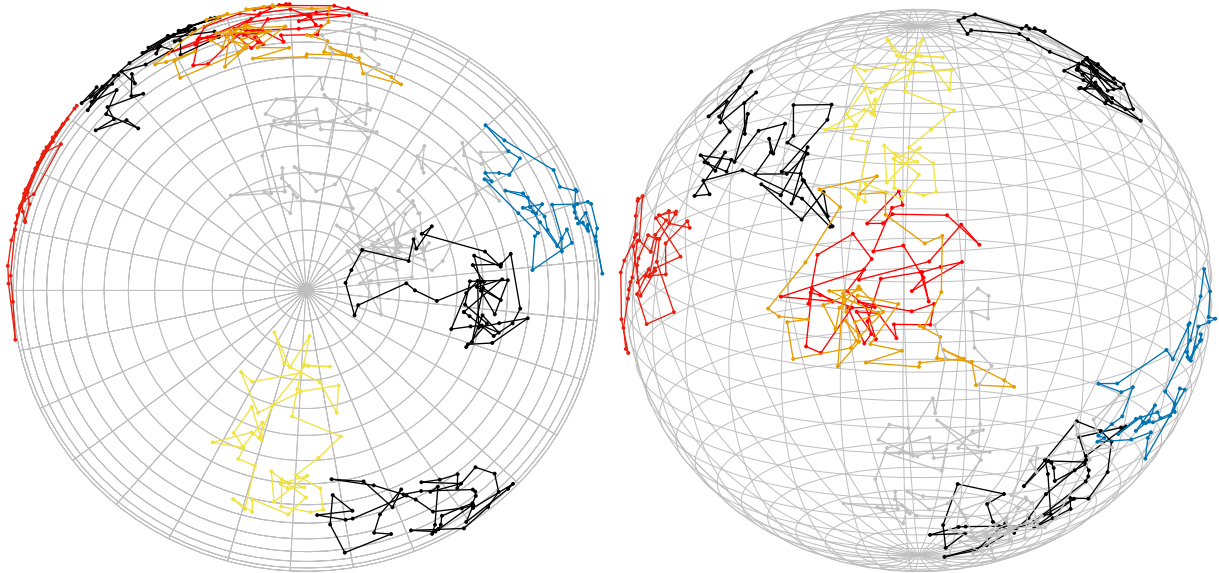


FIG. 1. Snapshot of the macroscopic path during the simulation for  $N = 10$  non interacting distinguishable particles with  $M = 50, a = 5, \beta = 10$ . Case A in Table I. The simulation started with all bodies distributed uniformly on the equator. The different paths have different colors. In the left panel the top view and in the right panel the front view. In the simulation we measured  $e_K = \langle \mathcal{K} \rangle = 1.089(4)$ . Reducing  $\beta$  each path shrinks and tends to form a ring enclosing less amount of area.

Many snapshots of the paths configurations during the simulation showed that the simulation “speed” of the beads of the paths near the poles gets small<sup>16</sup>. This should be a consequence of the hairy ball theorem mentioned in the introduction.

In Fig. 2 we show the radial distribution function, calculated by averaging the estimator of Eq. (3.5), for a gas of  $N = 10$  distinguishable non interacting particles on a sphere of radius  $a = 5$  at an inverse temperature  $\beta = 10$ . We used  $M = 50$  with only the displace move of appendix A (this was used for Fig. 1) and with both the displacement move and the bridge move of Appendix B. From the figure we see how both the simulation with only the displacement move and the one with both the displacement and the bridge move give the expected result  $g(r) = 1 - 1/N$ , where the  $1/N$  term takes care of the finite size of the system, for any  $M$ . This is a strong test on the correctness of our bridge move. We are then ready to use it for the permutations sampling necessary for identical particles. We will do this in the next section.

### B. Identical bodies

Here we use the Metropolis algorithm with the transition displacement moves of Eqs. (A1) and (A2) and bridge moves of Eqs. (B1) and (B2) between unlike particles as described in Appendix B to produce the necessary particles exchanges.

<sup>16</sup> In fact we have two different contributions responsible for this behavior: The  $g$  factor in the integration measure and the metric  $g_{\mu\nu}$  in the kinetic action. These cannot be removed with a change of coordinates since it would require a *non coordinate basis* [38].

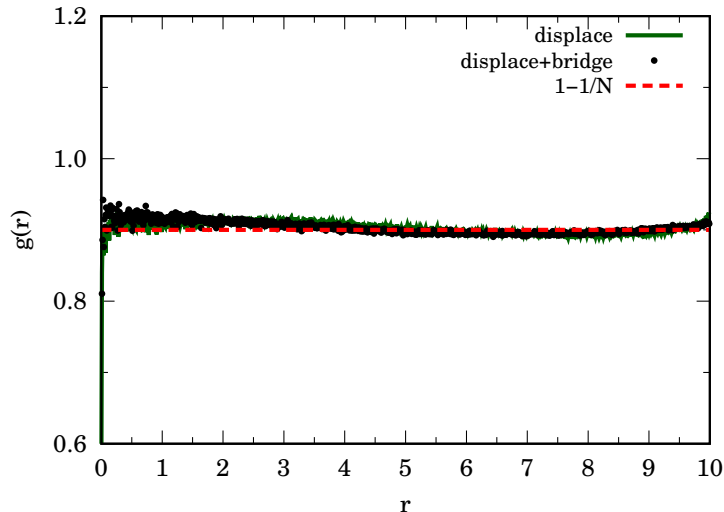


FIG. 2. The radial distribution function for the non interacting distinguishable particles gas with  $N = 10$  on a sphere of radius  $a = 5$  at an inverse temperature  $\beta = 10$ . We use  $M = 50$  (case A in Table I) with only the displace move of appendix A and with both the displace and the bridge move as described in Appendix B. The dashed line is for  $g(r) = 1 - 1/N = 0.9$ .

### Bosons

Given the *superfluid* density  $\sigma_s$  and the *normal fluid* density  $\sigma_n = 1 - \sigma_s$ , the area estimator for the superfluid fraction is given by [30, 45]

$$f_s = \frac{\sigma_s}{\sigma} = 1 - \frac{\sigma_n}{\sigma} = \frac{2m\langle \mathcal{A}^2 \rangle}{\beta\lambda I_c}, \quad (4.1)$$

where, if  $\epsilon$  is the Levi-Civita antisymmetric symbol,

$$\mathcal{A} = \frac{1}{2} \sum_{i,k} \epsilon_{\alpha\beta} (r_{i,k+1} - r_k)^\alpha (r_{i,k+2} - r_{k+1})^\beta \sqrt{g(\mathbf{r}_{i,k+1})}, \quad (4.2)$$

is the area occupied by all the single particle paths and  $I_c$  is the classical moment of inertia of the spherical shell that we will take as a fit parameter so that  $\lim_{\beta \rightarrow \infty} f_s = 1$ .

In Ref. [46] Nelson and Kosterlitz use renormalization method of Ref. [47] to study the behavior of the superfluid density defined in Ref. [48] at the superfluid phase transition. They found that the superfluid density  $\sigma_s$  undergoes a *universal* jump equal to,

$$\Delta\sigma_s = \frac{m^2}{\beta} \frac{2}{\pi}, \quad (4.3)$$

at the critical temperature,  $T_c$ , for the superfluid phase transition. This was also observed experimentally [49] for  $^4\text{He}$  films. In the present language this says that the average squared area has a jump of  $(I_c/\sigma)/2\pi$  at the transition. Naturally the phase transition can only occur in the thermodynamic limit which in our case would correspond to the case of a degenerate sphere of an infinite radius, i.e. flat.

In Fig. 3 we show the superfluid fraction of Eq. (4.1) for the condensate of non interacting bosons with  $N = 10$ ,  $a = 5$ ,  $M = 50$ .

In Fig. 4 we show a snapshot during the simulation for bosons non interacting particles with  $M = 50$ ,  $N = 10$ ,  $a = 5$ ,  $\beta = 100/3$ . We see how the system forms 5 permutation cycles corresponding to different colors.

In Fig. 5 we show the radial distribution function, calculated by averaging the estimator of Eq. (3.5), for the bosons non interacting gas with  $N = 10$  on a sphere of radius  $a = 5$  at an inverse temperature  $\beta = 100/3$  with  $M = 50$ . This is the same configuration used for Fig. 1. The bump at  $r = 0$  is a consequence of condensation predicted by the Bose-Einstein statistics which requires a symmetric density matrix respect to permutation of any two particles. Bosons like themselves [50] but on a sphere if they like themselves at one point they must form a hole on the opposite point.

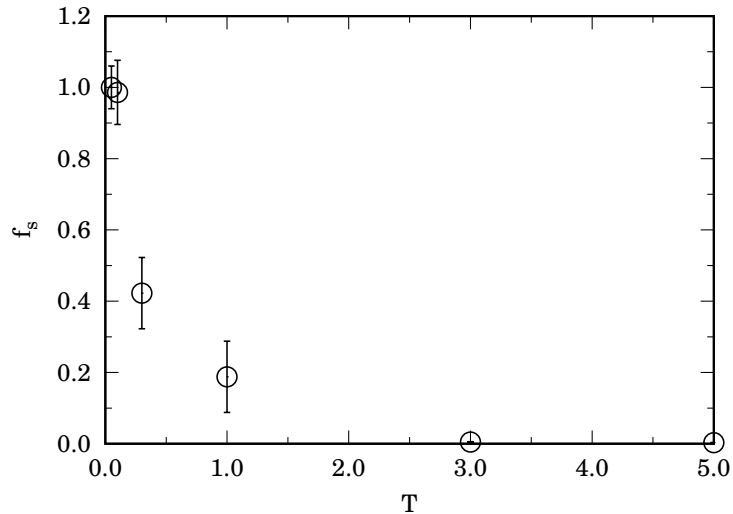


FIG. 3. The superfluid fraction (4.1) for the condensate of non interacting bosons with  $N = 10, a = 5, M = 50$ . In this case  $\tau \leq 0.4$  and  $T_c = T_D \approx 0.0318$ . The universal jump in  $f_s$  which would be expected at the superfluid phase transition is  $(4m^2 T_c / \sigma) / 2\pi \approx 0.636$ .

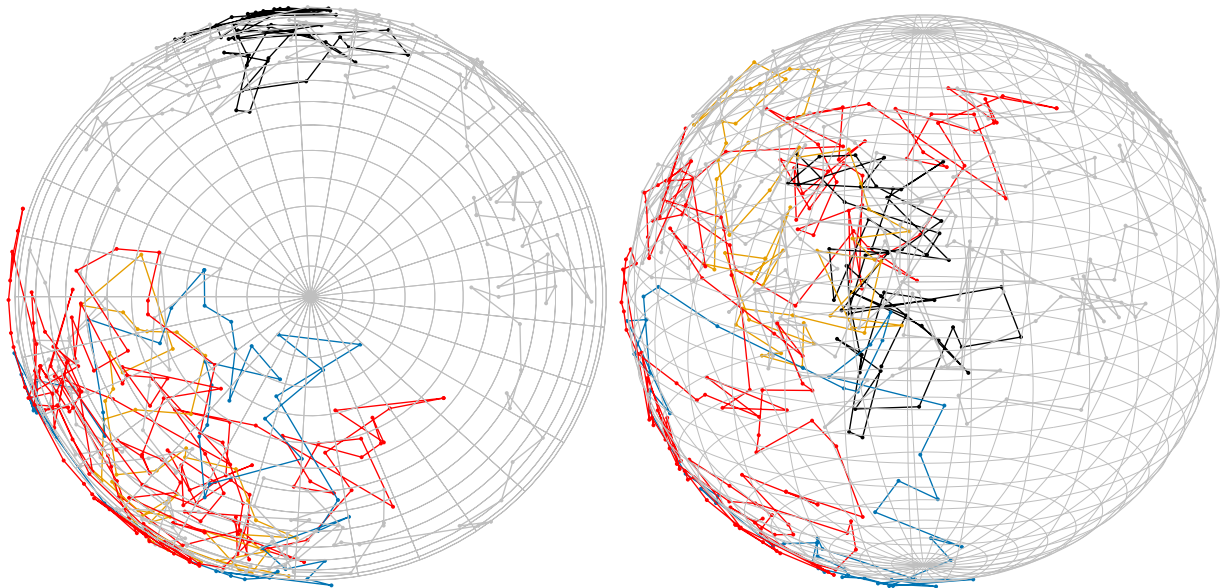


FIG. 4. Snapshot of the macroscopic path during the simulation for  $N = 10$  non interacting bosons with  $M = 50, a = 5, \beta = 100/3$ . Case B in Table I. The simulation started with all bodies distributed uniformly on the equator. Paths corresponding to different permutations cycles have different colors. In the left panel the top view and in the right panel the front view. In the simulation we measured  $e_K = \langle \mathcal{K} \rangle = 0.224(2)$ . Reducing  $\beta$  each path shrinks and tends to form a ring enclosing less amount of area.

### Fermions

Fermions properties cannot be calculated exactly with path integral Monte Carlo because of the *fermions sign problem* [39, 51]. We then have to resort to an approximated calculation. The one we chose was the Restricted Path Integral (RPIMC) approximation [3, 39, 50, 51] with a “free fermions restriction”. The trial density matrix used in the *restriction* is chosen as the one reducing to the ideal density matrix in the limit of  $t \ll 1$  and is given by the

following explicit analytic expression,

$$\rho_0(R', R; t) \propto \det \left\| e^{-\frac{s^2(\mathbf{r}'_i, \mathbf{r}_j)}{4\lambda t}} \right\|. \quad (4.4)$$

The *restricted path integral identity* that we will use states [39, 51]

$$\rho_-(R', R; \beta) \propto \int \sqrt{\tilde{g}''} dR'' \rho_-(R'', R; 0) \int_{R'' \rightarrow R' \in \gamma_0(R)} \mathcal{D}R''' e^{-S[R''']}, \quad (4.5)$$

where  $S$  is the Feynman-Kac action

$$S[R] = \int_0^\beta dt \left[ \frac{1}{4\lambda} \dot{R}_\mu \dot{R}^\mu + V(R) \right], \quad (4.6)$$

here the dot indicates a total derivative with respect to the imaginary thermal time, and the subscript in the path integral of Eq. (4.5) means that we restrict the path integration to paths starting at  $R''$ , ending at  $R'$  and avoiding the nodes of  $\rho_0$ , that is to the *reach* of  $R$ ,  $\gamma_0(R)$ .  $R$  will be called the *reference point* determining the reach. The nodes are on the reach boundary  $\partial\gamma_0$ . The weight of the walk is  $\rho_-(R'', R; 0) = \det \|\delta(\mathbf{r}''_i - \mathbf{r}_j)\|$ . Note that in imposing the restriction it is convenient to imagine an infinitely positive external potential which will prevent a transition move  $R \rightarrow R'$  such that  $\rho_0(R', R; \tau) < 0$ <sup>17</sup>. It is clear that the contribution of all the paths for a single element of the density matrix will be of the same sign, thus solving the sign problem; positive if  $\rho_-(R'', R; 0) > 0$ , negative otherwise. On the diagonal any density matrix is positive and on the path restriction  $\rho_-(R', R; \beta) > 0$ . Then only even permutations, those with  $\text{sgn}(\mathcal{P}) = +1$ , are allowed, since  $\rho_-(\mathcal{P}R, R; \beta) = \text{sgn}(\mathcal{P})\rho_-(R, R; \beta)$ . It is then possible to use a bosons calculation to get the fermions case. Clearly the restricted path integral identity with the free fermions restriction becomes exact if we simulate free fermions, but otherwise is just an approximation.

The restriction implementation is rather simple: we just reject the move whenever the proposed path is such that the ideal fermion density matrix (4.4) calculated between the reference point and any of the time slices subject to newly generated particles positions has a negative sign. So in correspondence of each displace move of Appendix A or bridge move of Appendix B it is necessary to calculate  $M$  determinants of order  $N$ . For this reason the method becomes unfeasible to treat systems with very many particles. To increase the acceptances in the restrictions, we found it convenient to choose the reference point time slice randomly, i.e. we choose an integer random number between 1 and  $M$ , say  $m$ , and the reference point is chosen to be  $R = R_m$ , before each move. This is allowed because we are free to perform a translation in the  $\beta$ -periodic imaginary thermal time.

In Fig. 5 we show the radial distribution function, calculated by averaging the estimator of Eq. (3.5), for the non interacting, spinless,  $g_s = 1$ , fermions gas with  $N = 10$  on a sphere of radius  $a = 5$  at an inverse temperature  $\beta = 100/3$  with  $M = 50$ . This is case C of Table I. The well at  $r = 0$  is a consequence of Pauli exclusion principle predicted by the Fermi-Dirac statistics which requires an antisymmetric density matrix respect to permutaion of any two particles. This well is usually called *exchange hole*. Fermions dislike themselves [50] but on a sphere if they dislike themselves at one point they must form a bump on the opposite point. A simple sum rule in this case requires  $g(0) = 0$  since the the density matrix for coincident particles is singular and its determinant must be zero.

### Anyons

Here we use the Metropolis algorithm with the transition displacement moves of Eqs. (A1) and (A2) and the swap moves of Eqs. (B1) and (B2) between two particles, as described in Appendix C, counting at each swap move the number of single particles crossings  $n$  in the newly generated path  $R$ .

For example, from Eqs. (2.19)-(2.20) follows that, for  $\nu = 1/2$ ,

$$\text{Re}[\chi(\alpha)] = \begin{cases} (-1)^k & n = 2k \\ 0 & n = 2k + 1 \end{cases} \quad k = 0, 1, 2, 3, \dots \quad (4.7)$$

We then see that in order to calculate  $\rho_{1/2}$  necessary to simulate anyonic statistics for  $\nu = 1/2$ , one can simply use the RPIMC described above, i.e. a bosons PIMC with a restriction based on the nodes of the reference trial density matrix of Eq. (4.4), as for fermions, but now we simply have to additionally throw away those moves that generate

<sup>17</sup> So that a move that changes the sign of  $\rho_0$  are rejected in the Metropolis scheme.

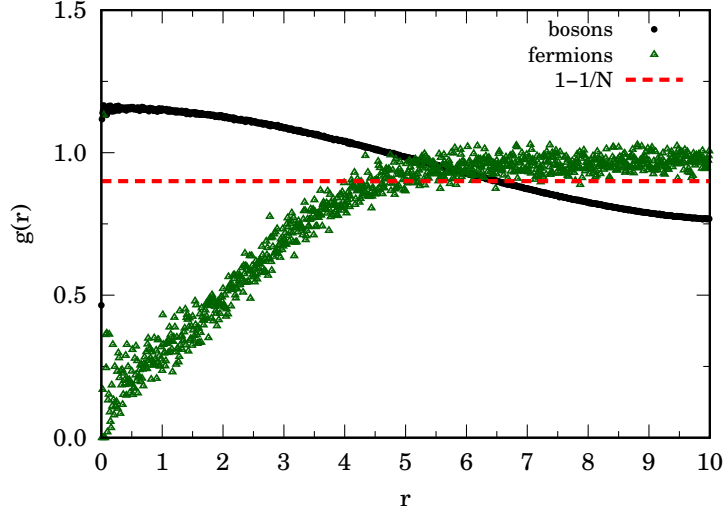


FIG. 5. The radial distribution function for the non interacting bosons and fermions gas with  $N = 10$  on a sphere of radius  $a = 5$  at an inverse temperature  $\beta = 100/3$  with  $M = 50$ . Case B and C in Table I respectively. The dashed line is for  $g(r) = 1 - 1/N = 0.9$ . The bump at  $r = 0$  for bosons is a manifestation of their tendency to like themselves. The exchange hole at  $r = 0$  for fermions is a manifestation of their tendency to dislike themselves due to the Pauli exclusion principle and it requires  $g(0) = 0$ .

an odd number  $n$  of single particles crossings. Once again, as long as, we have no interaction between the anyonic particles this scheme is expected to give rise to an exact computation. In order to count the number  $n$  of braids we can proceed as described in Appendix C.

In Fig. 6 we show the radial distribution function, calculated by averaging the estimator of Eq. (3.5), for the non interacting,  $\nu = 1/2$ , anyons gas with  $N = 10$  on a sphere of radius  $a = 5$  at an inverse temperature  $\beta = 100/3$  with  $M = 50$ . This is case D of Table I. We compare it with the radial distribution for non interacting fermions already shown in Fig. 5. From the comparison we can say that there is no difference in the structure of the two fluids. We can then say that all  $\nu = q/2$  with  $q = 1, 2, 3, \dots$  correspond to the same class.

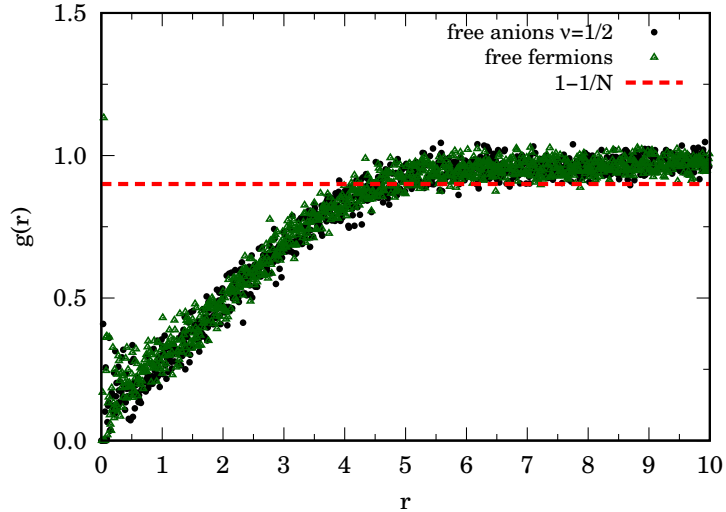


FIG. 6. The radial distribution function for the non interacting  $\nu = 1/2$  anyons gas with  $N = 10$  on a sphere of radius  $a = 5$  at an inverse temperature  $\beta = 100/3$  with  $M = 50$ . Case D in Table I respectively. The dashed line is for  $g(r) = 1 - 1/N = 0.9$ .

We suspect that fractional statistics  $\nu = q/p$  with  $0 < q < p$  will in general result in fluids with different structure.

For example, for  $\nu = 1/3$  we would find

$$\text{Re}[\chi(\alpha)] = \begin{cases} (-1)^k & n = 3k \\ (-1)^k \cos(\pi/3) & n = 3k + 1 \\ (-1)^k \cos(2\pi/3) & n = 3k + 2 \end{cases} \quad k = 0, 1, 2, 3, \dots \quad (4.8)$$

and the case  $\nu = 2/3$  should differ from the  $\nu = 1/3$  case. It would also be interesting to explore other rational cases  $\nu = q/p$  with  $0 < \nu < 1$  and see whether their structure differs from the irrational cases.

## V. ELECTRON GAS

In this section we will study a system of electrons, i.e. fermions interacting through the Coulomb potential of Eq. (3.4) with  $e = 1$ . We will only consider the spinless  $s = 0, g_s = 1$  case where the density matrix is antisymmetric respect to permutation of any two particles. In this case we are unable to solve exactly the problem even numerically with PIMC due to the fermions sign problem described above. We will use the RPIMC with the ideal free fermions restriction based on the nodes of the reference density matrix of Eq. (4.4). This strategy is exact for non interacting fermions and is here expected to become a better approximation at low density and high temperature, i.e. when correlation effects are weak.

In Fig. 7 we show the radial distribution function for the electron gas of case E in Table I. From the figure we see how the gas develops a *correlation hole* at  $r = 0$  in addition to the exchange hole shown in Fig. 5. The radial distribution goes to zero at the origin,  $r = 0$ , and develops oscillations beyond  $r \approx 5$ .

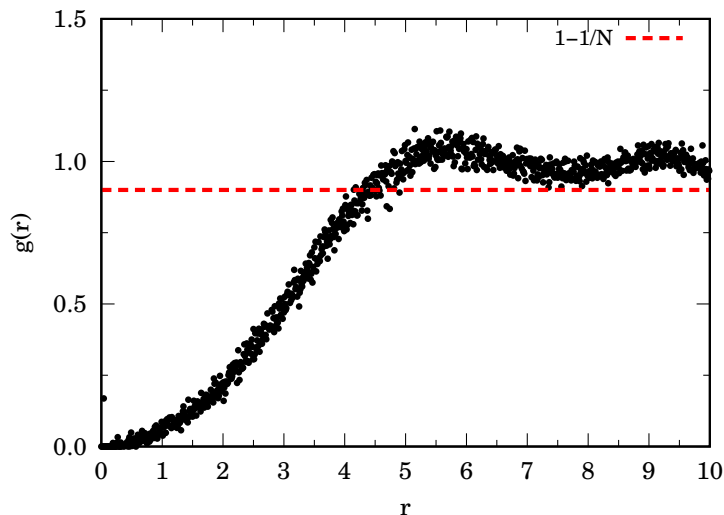


FIG. 7. The radial distribution function for the spinless electron gas interacting through the Coulomb potential of Eq. (3.4) with  $e = 1$ . We show case E of Table I where we have  $N = 10$  electrons on a sphere of radius  $a = 5$  at an inverse temperature  $\beta = 100/3$  with  $M = 50$ . The radial distribution shown an *exchange-correlation hole* in a neighborhood of  $r = 0$  and oscillations beyond  $r \approx 5$ .

## VI. CONCLUSIONS

In this work we studied the effect of a constant positive curvature on a two dimensional quantum many body fluid. This is the simplest case that can be thought of in an exploration of the influence of curvature on the surface where the bodies move. At sufficiently low temperature quantum effects become important and the fluid will behave differently depending on the statistics ruling the bodies. The statistics depends on the transformation property of the many body wavefunction under exchange of two bodies. If the bodies are distinguishable the wavefunction and its transformed will be different, if they are identical the transformed wavefunction can only be plus or minus the original wavefunction. The plus will be for bodies obeying to Bose-Einstein statistics and the minus for bodies obeying

to the Fermi-Dirac statistics. If the identical bodies are also impenetrable the transformed wavefunction can more generally be the original wavefunction times a phase factor  $e^{i\nu\pi}$  since, on a surface, exchanging the two particles by a clockwise rotation of  $\pi$  around their center of mass is a topologically and physically distinct operation than rotating counterclockwise. In this case the bodies are said to obey to the anyonic statistics, where the statistics is determined by the phase  $\nu$ . For  $\nu = 0$  (modulo 2) one recovers the bosonic statistics and for  $\nu = 1$  (modulo 2) the fermionic statistics. While for bosons and fermions just the permutation of the particles in their initial and final configuration in imaginary time matters, for anyons it is also necessary to specify how the different trajectories wind or *braid* around each other. In other words the imaginary time evolution of the particles matters and cannot be neglected. The representation of the permutation group must be replaced by the one of the braid group.

We made some computer experiments for each one of these cases using a PIMC algorithm different from the one previously used in Ref. [3, 4]. For the sign problem hidden in the Fermi-Dirac and the anyonic statistics we then used the RPIMC method. We studied both the case of the non interacting bodies and for the fermions case the electron gas with a three dimensional pair Coulomb interaction depending on the Euclidean distance between two electrons. In each case we measured the kinetic energy, the potential energy, and the radial distribution function. The pair correlation function of non interacting fermions displays, at contact, the exchange hole and the one of the electron gas displays the exchange-correlation hole. While fermions dislike themselves due to the Pauli exclusion principle, bosons like themselves and form a condensate. This is reflected in a bump in the pair correlation function at contact. For bosons we also measured the superfluid fraction using an area estimator devised by Pollock and Ceperley and confirm its universal jump at the superfluid transition, as predicted by Nelson and Kosterlitz.

During our simulations we made various snapshots of the many body path configuration and we noticed that the simulation “speed” of the single particle beads in proximity of the poles diminishes. We explained this occurrence as a consequence of the metric tensor properties which affect both the kinetic action and the path integral measure.

For the case of anyons we only considered the fractional statistics  $\nu = 1/2$ . It would be interesting to understand whether in the transition from a rational to an irrational statistics, there is any macroscopic observable change in the structure of the anyons fluid.

We plan in the future to measure the effect of curvature on the pressure of the fluid as was done in the non quantum case in Ref. [19].

### Appendix A: The transition displacement move

In order to explore the  $\theta$  and  $\varphi$  positions space  $\mathcal{C} = ]-\pi/2, \pi/2] \times ]-\pi, \pi]$  on the sphere it is convenient to propose the following transition move for each particle in a randomly chosen bead

$$\theta_{\text{new}} = \theta_{\text{old}} + \Delta_{\theta}(\eta - 1/2), \quad (\text{A1})$$

$$\varphi_{\text{new}} = \varphi_{\text{old}} + \Delta_{\varphi}(\eta - 1/2), \quad (\text{A2})$$

where  $\eta \in [0, 1]$  is a uniform pseudo random number and  $\Delta_{\theta}$  and  $\Delta_{\varphi}$  are two positive quantities measuring the  $\theta$ -displacement and the  $\varphi$ -displacement respectively.

This transition move can bring  $\mathbf{r}_{\text{new}}$  out of  $\mathcal{C}$  so it is also necessary to bring it back into  $\mathcal{C}$  enforcing periodic boundary conditions  $\varphi = \varphi + 2\pi$  and  $\theta = \theta + \pi$  with the following subsequent chain of transformations

$$\begin{cases} \theta_{\text{new}} \rightarrow \theta_{\text{new}} - \pi \text{NINT}(\theta_{\text{new}}/\pi), \\ \varphi_{\text{new}} \rightarrow \varphi_{\text{new}} - 2\pi \text{NINT}(\varphi_{\text{new}}/2\pi), \end{cases} \quad (\text{A3})$$

where NINT is the nearest integer function. One can easily convince himself that this chain does not alter the uniformity of the probability distribution of  $\mathbf{r}_{\text{new}}$  in  $\mathcal{C}$ .

Note that the metric enters the free particle variance since it is not possible by a change of coordinates to remove it both from the kinetic-action and from the integration measure  $\sqrt{g(\mathbf{r})} d\mathbf{r}$ , if not only locally. In order to take care of the metric factor in the integration measure it is convenient to introduce an effective/external single particle potential  $\ln \sqrt{g(\mathbf{r})}$ .

In the simulation we choose  $\Delta_{\theta}$  and  $\Delta_{\varphi}$  so to have acceptance ratios as close as possible to 1/2 in the acceptance/rejection choices for the random walk transition displacement moves of the Metropolis algorithm. The transition probability distribution function for the displacement move of the Metropolis algorithm will be uniform so it will drop out of the acceptance probability distribution function.

## Appendix B: The transition bridge move

In order to take into account the particles permutations it is necessary to construct two Brownian bridges between two different <sup>18</sup> randomly chosen particles in two randomly chosen beads to generate an exchange between the two particles. With one bridge we connect particle 1 on bead  $R_i$  to particle 2 on bead  $R_j$  and with the other we connect particle 2 on bead  $R_i$  to particle 1 on bead  $R_j$  with  $i < j$ . This will produce an exchange of particles 1 and 2.

The Brownian bridge between particle 1 at  $\mathbf{r}_{1,i}$  and particle 2 at  $\mathbf{r}_{2,j}$  is built through the following multislice transition move [30],

$$\mathbf{x}_{\text{new},i} = \mathbf{x}_{1,i} \tag{B1}$$

$$\mathbf{x}_{\text{new},k} = \mathbf{x}_{\text{new},k-1} + \frac{\mathbf{x}_{2,j} - \mathbf{x}_{\text{new},k-1}}{j - k + 1} + \xi \quad k = i + 1, \dots, j \tag{B2}$$

where  $\mathbf{x} = (\mathcal{X}, \mathcal{Y})$  is a two dimensional vector on a flat space and  $\xi$  is a random number with a Gaussian probability distribution <sup>19</sup> with zero mean and variance  $\sigma^2(j-k)/(j-k+1)$  where  $\sigma^2 = 2\lambda\tau$  is the diagonal free particle variance. We will then first perform a direct mapping  $\theta \rightarrow \mathcal{X}$  and  $\varphi \rightarrow \mathcal{Y}$ . Then the bridge move of Eqs. (B1)-(B2). And finally we go back to the sphere with the inverse mapping  $\mathcal{X} \rightarrow \theta$  and  $\mathcal{Y} \rightarrow \varphi$ . We will then have a direct mapping of the many body system  $R \rightarrow X = (\mathbf{x}_1, \mathbf{x}_2, \dots, \mathbf{x}_N) = (\{\mathbf{x}_i\})$  and an inverse mapping  $X \rightarrow R$  back on the sphere.

The Metropolis (rejection) method can sample any probability distribution provided that the transition rule satisfies detailed balance and ergodicity. The Metropolis algorithm is a particular way of ensuring that the transition rule satisfies detailed balance. It does this by splitting the transition probability into an ‘‘a priori’’ *sampling distribution*  $T(s \rightarrow s')$  (which is a probability distribution that we can sample) and an *acceptance probability*  $A(s \rightarrow s')$  where  $0 \leq A \leq 1$ .

$$P(s \rightarrow s') = T(s \rightarrow s')A(s \rightarrow s'), \tag{B3}$$

In the generalized Metropolis procedure [42], trial moves are accepted according to:

$$A(s \rightarrow s') = \min[1, q(s \rightarrow s')], \tag{B4}$$

where

$$q(s \rightarrow s') = \frac{\pi(s')T(s' \rightarrow s)}{\pi(s)T(s \rightarrow s')}. \tag{B5}$$

where  $\pi \propto e^{-\mathcal{S}}$  is the action probability distribution in the  $s = (\{R_k\}, \mathcal{P})$  configurations space. The transition probability corresponding to the move of Eqs. (B1)-(B2) is then given by

$$\frac{T(s_{\text{new}} \rightarrow s_{\text{old}})}{T(s_{\text{old}} \rightarrow s_{\text{new}})} \propto \exp \left[ \sum_{k=i+1}^j (X_{\text{new},k} - X_{\text{new},k-1})^2/4\lambda\tau - \sum_{k=i+1}^j (X_{\text{old},k} - X_{\text{old},k-1})^2/4\lambda\tau \right]. \tag{B6}$$

So we start from  $R_{\text{old}}$  map it to  $X_{\text{old}}$ , on the direct mapping flat space perform the Brownian bridge move, accept or reject the transition according to the probability (B4) to find  $X_{\text{new}}$ , and finally inverse map it back to  $R_{\text{new}}$  on the sphere. Ergodicity in  $\mathcal{Y}$  would be lost only if we are *exactly* on a pole. But this is always prevented on a computer due to the finite arithmetic! Moreover since we have ergodicity everywhere in  $\mathcal{X}$  it will always be possible to escape a pole by moving along  $\mathcal{X}$ .

In order to produce an exchange of two particles 1 and 2 one needs a two combined bridge transitions as described above. Any permutation can be reached through a two particles exchange so the bridge transition move allows to sample the sum in Eq. (2.17).

## Appendix C: Braids sampling

In order to sample the sum in Eq. (2.19) one needs a move able to bring the path  $R(t)$  from one homotopy class to another. And a way to understand to which homotopy class the path belongs after each move. This will allow one to determine to which  $\rho_\alpha$  he is contributing at each accepted transition move.

<sup>18</sup> A bridge between the same particle can still be used to sample the density matrix of distinguishable particles as can be done the displacement move of Appendix A.

<sup>19</sup> This can be generated with the Box-Muller algorithm [42] for example.

A path  $R(t)$  made of closed distinct single particle paths,  $\mathbf{r}(0) = \mathbf{r}(\beta)$ , on a sphere, can only have an even number  $n$  of two particles crossings, i.e. of braids. Allowing for particles exchanges  $n$  can be any integer. If two different particles, say 1 and 2, have  $m$  crossings between timeslices  $k_i$  and  $k_f$ , an acceptance of the swap move described in Appendix B, will necessarily result in a single crossing if  $m$  is even, and consequently  $n \rightarrow n - m + 1$ , or to no crossing at all, if  $m$  is odd, and consequently  $n \rightarrow n - m$ .

We see then how we can use the swap move to jump from any homotopy class to any another. And within an homotopy class  $\alpha$  we can then act with the displace move described in Appendix A to sample  $\rho_\alpha$ .

In order to count the number of crossings between particles 1 and 2 between timeslices  $k_i$  and  $k_f$  it is necessary to count the number of times in which  $\mathbf{r}_{1,k} = \mathbf{r}_{2,k}$  for  $k \in [k_i, k_f]$ . In order to take into account of this crossing condition in the discretized imaginary time one can for example determine when both  $r_{1,k}^\alpha - r_{2,k}^\alpha$  for  $\alpha = 1, 2$  change sign or are zero, varying  $k$ . Counting the number  $n$  of braids reached in the path  $R(t)$  allows to asses to which path homotopy class one is contributing in the density matrix.

## AUTHOR DECLARATIONS

### Conflicts of interest

None declared.

### Data availability

The data that support the findings of this study are available from the corresponding author upon reasonable request.

### Funding

None declared.

- 
- [1] J. R. Klauder and R. Fantoni, The Magnificent Realm of Affine Quantization: valid results for particles, fields, and gravity, *Axioms* **12**, 911 (2023).
  - [2] R. Fantoni, *Unifying Classical and Quantum Physics - How classical and quantum physics can pass smoothly back and forth* (Springer, New York, 2025).
  - [3] R. Fantoni, One-component fermion plasma on a sphere at finite temperature, *Int. J. Mod. Phys. C* **29**, 1850064 (2018).
  - [4] R. Fantoni, One-component fermion plasma on a sphere at finite temperature. The anisotropy in the paths conformations, *J. Stat. Mech.* , 083103 (2023).
  - [5] G. O. V. Melik-Alaverdian, N. E. Bonesteel, Fixed-phase diffusion Monte Carlo study of the quantum-Hall effect on the Haldane sphere, *Physica E* **1**, 138 (1997).
  - [6] G. O. V. Melik-Alaverdian, N. E. Bonesteel, Quantum Hall Fluids on the Haldane Sphere: A Diffusion Monte Carlo Study, *Phys. Rev. Lett.* **79**, 5286 (1997).
  - [7] N. E. B. V. Melik-Alaverdian, G. Ortiz, Quantum Projector Method on Curved Manifolds, *Phys. Rev. Lett.* 10.48550/arXiv.cond-mat/0001121 (1997), arXiv:cond-mat/0001121.
  - [8] J. Ginibre, Statistical Ensembles of Complex, Quaternion, and Real Matrices, *J. Math. Phys.* **6**, 440 (1965).
  - [9] M. L. Metha, *Random Matrices* (Academic, New York, 1967).
  - [10] B. Jancovici, Exact Results for the Two-Dimensional One-Component Plasma, *Phys. Rev. Lett.* **46**, 386 (1981).
  - [11] A. Alastuey and B. Jancovici, On the classical two-dimensional one-component Coulomb plasma, *J. Phys. (France)* **42**, 1 (1981).
  - [12] P. Choquard, *Helv. Phys. Acta* **54**, 332 (1981).
  - [13] P. Choquard, P. J. Forrester, and E. R. Smith, The two-dimensional one-component plasma at  $\Gamma = 2$ : The semiperiodic strip, *J. Stat. Phys.* **33**, 13 (1983).
  - [14] J. M. Caillol, Exact results for a two-dimensional one-component plasma on a sphere, *J. Phys. (France) - Lett.* **42**, L (1981).
  - [15] G. Téllez and P. J. Forrester, Exact Finite-Size Study of the 2D OCP at  $\Gamma = 4$  and  $\Gamma = 6$ , *J. Stat. Phys.* **97**, 489 (1999).
  - [16] B. Jancovici, Pressure and Maxwell Tensor in a Coulomb Fluid, *J. Stat. Phys.* **99**, 1281 (2000).

- [17] R. P. Salazar and G. Téllez, Exact Energy Computation of the One Component Plasma on a Sphere for Even Values of the Coupling Parameter, *J. Stat. Phys.* **164**, 969 (2016).
- [18] B. Jancovici and G. Téllez, Two-Dimensional Coulomb Systems on a Surface of Constant Negative Curvature, *J. Stat. Phys.* **91**, 953 (1998).
- [19] R. Fantoni, B. Jancovici, and G. Téllez, Pressures for a One-Component Plasma on a Pseudosphere, *J. Stat. Phys.* **112**, 27 (2003).
- [20] B. Jancovici and G. Téllez, Charge Fluctuations for a Coulomb Fluid in a Disk on a Pseudosphere, *J. Stat. Phys.* **116**, 205 (2004).
- [21] R. Fantoni and G. Téllez, Two dimensional one-component plasma on a Flamm's paraboloid, *J. Stat. Phys.* **133**, 449 (2008).
- [22] R. Fantoni, Two component plasma in a Flamm's paraboloid, *J. Stat. Mech.* , P04015 (2012).
- [23] E. Artin, Theory of Braids, *Annals of Mathematics* **48**, 101 (1947).
- [24] R. Fantoni, J. W. O. Salari, and B. Klumperman, The structure of colloidosomes with tunable particle density: Simulation vs experiment, *Phys. Rev. E* **85**, 061404 (2012).
- [25] H. Poincaré, Sur les courbes définies par les équations différentielles, *Journal de Mathématiques Pures et Appliqués* **4**, 167 (1885).
- [26] L. E. J. Brouwer, Über Abbildung von Mannigfaltigkeiten, *Mathematische Annalen* **71**, 97 (1912).
- [27] H. Hopf, Vektorfelder in n-dimensionalen Mannigfaltigkeiten, *Math. Ann.* **96**, 209 (1926).
- [28] F. Bastianelli and O. Corradini, On the simplified path integral on spheres, *Eur. Phys. J. C* **77**, 731 (2017).
- [29] E. Artin, Ein mechanisches System mit quasi-ergodischen Bahnen, *Abh. Math. Sem. d. Hamburgischen Universität* 10.1007/BF02954622 (1924).
- [30] D. M. Ceperley, Path integrals in the theory of condensed Helium, *Rev. Mod. Phys.* **67**, 279 (1995).
- [31] R. Fantoni, Statistical Gravity through Affine Quantization, *Quantum Rep.* **6**, 706 (2024).
- [32] R. Fantoni, Statistical Gravity and entropy of spacetime, *Stats* **8**, 23 (2025).
- [33] R. Fantoni, Statistical Gravity, ADM splitting, and Affine Quantization, *Gravitation and Cosmology* **31**, 568 (2025).
- [34] B. S. DeWitt, Dynamical Theory in Curved Spaces. I. A Review of the Classical and Quantum Action Principles, *Rev. Mod. Phys.* **29**, 377 (1957).
- [35] J. H. V. Vleck, The Correspondence Principle in the Statistical Interpretation of Quantum Mechanics, *Proc Natl Acad Sci U S A* **14**, 178 (1928).
- [36] L. S. Schulman, *Techniques and Applications of Path Integration* (John Wiley & Sons, Technion, Haifa, Israel, 1981) chapter 24.
- [37] H. F. Trotter, On the Product of Semi-Groups of Operators, *Proc. Am. Math. Soc.* **10**, 545 (1959).
- [38] C. W. Misner, K. S. Thorne, and J. A. Wheeler, *Gravitation* (W. H. Freeman, San Francisco, 1973).
- [39] D. M. Ceperley, Path integral Monte Carlo methods for fermions, in *Monte Carlo and Molecular Dynamics of Condensed Matter Systems*, edited by K. Binder and G. Ciccotti (Editrice Compositori, Bologna, Italy, 1996).
- [40] A. Lerda, *Anyons. Quantum Mechanics of Particles with Fractional Statistics* (Springer-Verlag, Berlin, 1992).
- [41] N. Metropolis, A. W. Rosenbluth, M. N. Rosenbluth, A. M. Teller, and E. Teller, Equation of state calculations by fast computing machines, *J. Chem. Phys.* **1087**, 21 (1953).
- [42] M. H. Kalos and P. A. Whitlock, *Monte Carlo Methods* (John Wiley & Sons Inc., New York, 1986).
- [43] E. A. Abbott, *Flatland: A Romance of Many Dimensions* (Seeley & Co., London, 1884).
- [44] R. Fantoni, Plasma living in a curved surface at some special temperature, *Physica A* **177**, 524 (2019).
- [45] E. L. Pollock and D. M. Ceperley, Path-integral computation of superfluid densities, *Phys. Rev. B* **36**, 8343 (1987).
- [46] D. R. Nelson and J. M. Kosterlitz, Universal Jump in the Superfluid Density of Two-Dimensional Superfluids, *Phys. Rev. Lett.* **39**, 1201 (1977).
- [47] J. U. José, L. P. Kadanoff, S. Kirkpatrick, and D. R. Nelson, Renormalization, vortices, and symmetry-breaking perturbations in the two-dimensional planar model, *Phys. Rev. B* **16**, 1217 (1977).
- [48] R. P. Feynmann, Application of Quantum Mechanics to Liquid Helium, *Prog. Low Temp. Phys.* **1**, 17 (1955).
- [49] J. Bishop and J. D. Reppy, Study of the Superfluid Transition in Two-Dimensional  $^4\text{He}$  Films, *Phys. Rev. Lett.* **40**, 1727 (1978).
- [50] R. Fantoni, Jellium at finite temperature, *Mol. Phys.* **120**, 4 (2021).
- [51] D. M. Ceperley, Fermion Nodes, *J. Stat. Phys.* **63**, 1237 (1991).